

LETTER

Variations of leaf longevity in tropical moist forests predicted by a trait-driven carbon optimality model

Xiangtao Xu,^{1*} David Medvigy,^{1,2}
 Stuart Joseph Wright,³
 Kaoru Kitajima,^{3,4} Jin Wu,⁵
 Loren P. Albert,⁶
 Giordane A. Martins,⁷
 Scott R. Saleska,⁶ and
 Stephen W. Pacala⁸

Abstract

Leaf longevity (LL) varies more than 20-fold in tropical evergreen forests, but it remains unclear how to capture these variations using predictive models. Current theories of LL that are based on carbon optimisation principles are challenging to quantitatively assess because of uncertainty across species in the ‘ageing rate,’ the rate at which leaf photosynthetic capacity declines with age. Here, we present a meta-analysis of 49 species across temperate and tropical biomes, demonstrating that the ageing rate of photosynthetic capacity is positively correlated with the mass-based carboxylation rate of mature leaves. We assess an improved trait-driven carbon optimality model with *in situ* LL data for 105 species in two Panamanian forests. We show that our model explains over 40% of the cross-species variation in LL under contrasting light environment. Collectively, our results reveal how variation in LL emerges from carbon optimisation constrained by both leaf structural traits and abiotic environment.

Keywords

Carbon optimisation, functional trait, leaf ageing, leaf economics spectrum, leaf longevity, modelling, photosynthesis.

Ecology Letters (2017) 20: 1097–1106

INTRODUCTION

Leaf longevity (LL) is a critical plant trait closely linked to plant resource use, phenology and growth strategy (Wright *et al.* 2004; Wu *et al.* 2016). In tropical forests, there is remarkable diversity in LL across species, ranging from several weeks to 6 years or more (Reich *et al.* 1991; Russo & Kitajima 2016). In addition, LL exhibits substantial phenotypic plasticity within the same species, including high sensitivity to variations in light environment (Williams *et al.* 1989; Lusk *et al.* 2008; Kitajima *et al.* 2013; Russo & Kitajima 2016). These variations in LL are associated with variations of other leaf traits, including leaf mass per area (LMA) and maximum carbon assimilation rate as described by the leaf economics spectrum (Wright *et al.* 2004).

A common theory to explain variations in LL regards LL as an outcome of plant strategy to optimise carbon gain (Chabot & Hicks 1982) or the associated plant water use (Blonder *et al.* 2011). Previous studies have proposed carbon optimality models at both leaf level (Kikuzawa 1991) and canopy level (Ackerly 1999; McMurtrie & Dewar 2011). These models provide theoretical basis to explain the leaf economics spectrum. Here, we focus on the foundational leaf-level optimality model. The leaf-level model searches the optimal LL that maximises average carbon gain per unit time. Based on the

assumptions that (1) plants can produce new leaves at any time of year, (2) leaf construction cost is a one-time investment at leaf production and (3) daily carbon gain is maximal when leaves are young and declines approximately linearly as leaves age, Kikuzawa (1991) predicts:

$$LL = \sqrt{\frac{2b \times CC \times LMA}{A_a}}, \quad (1)$$

where LL (day) denotes the optimal LL, A_a ($\text{g m}^{-2} \text{ day}^{-1}$) is daily carbon assimilation rate per leaf area when leaf age is zero, b (day) is the age when daily carbon assimilation rate would be reduced to zero, LMA (g m^{-2}) is LMA and CC (gC gC^{-1}) denotes the carbon construction cost per unit leaf mass carbon. In eqn 1, LL varies positively with LMA and negatively with A_a , which is supported by the leaf economics spectrum (Wright *et al.* 2004). However, we contend that the accuracy and practical applicability of eqn 1 are limited in several respects.

First, the covariation of plant functional traits is often ignored or poorly represented when LL is modelled. For example, the decline rate of photosynthetic capacity during leaf ageing (the inverse of b in eqn 1, referred to as ‘leaf ageing rate’ here after) covaries with LMA and photosynthetic capacity (Kitajima *et al.* 1997; Kikuzawa & Lechowicz 2006).

¹Department of Geosciences, Princeton University, Princeton, NJ 08544, USA

²Department of Biological Sciences, University of Notre Dame, Notre Dame, IN 46556, USA

³Smithsonian Tropical Research Institute, Apartado, Balboa 0843-03092, Panama

⁴Graduate School of Agriculture, Kyoto University, Kyoto 606-8502, Japan

⁵Environmental & Climate Sciences Department, Brookhaven National Laboratory, Upton, New York, NY 11973, USA

⁶Department of Ecology and Evolutionary Biology, University of Arizona, Tucson, AZ 85721, USA

⁷National Institute of Amazonian Research – INPA, Petrópolis, Brazil

⁸Department of Ecology and Evolutionary Biology, Princeton University, Princeton, NJ 08544, USA

*Correspondence

E-mail: xu.withoutwax@gmail.com

Quantifying this trait covariation will allow us to infer leaf ageing rate, which is often difficult to measure (Osada *et al.* 2015), and improve the accuracy of the carbon optimality model for LL (Kikuzawa *et al.* 2013).

Second, it is difficult to incorporate the effects of the abiotic environment on daily carbon gain in eqn 1. For example, the light gradient from the canopy to the deeply shaded understory must be incorporated to accurately assess leaf carbon economy in tropical forests. Kikuzawa *et al.* (2004) addressed this problem by estimating mean labour time of a leaf, which is the ratio of realised daily carbon gain to potential carbon gain rate. However, mean labour time cannot be directly measured and its value is difficult to determine because it varies greatly across species and environments (Kikuzawa & Lechowicz 2006). A potentially more accurate way to assess leaf carbon gain involves using biochemical photosynthesis models to capture leaf-specific response of daily carbon gain to environmental variations (Falster *et al.* 2012).

Third, construction costs based only on biochemical energy and materials required to build the leaf may be underestimated. From a whole-plant perspective, construction cost also includes petioles and branches that hold the leaf, the associated growth respiration (Kikuzawa & Ackerly 1999), the costs of nutrient acquisition and buds and young leaves lost to herbivory (Coley & Barone 1996). Ignoring these plant-level costs would create a negative bias in the predicted optimal LL.

Together, these problems can limit the predictive power of the LL optimality model. However, evaluation of the optimality model is lacking in tropical forests. The objective of this study is to rigorously test how well the leaf-level optimality theory can explain the variation in LL observed in tropical forests. To achieve this goal, we improve the optimality model by incorporating a mechanistic biochemical photosynthesis module that can realistically account for leaf abiotic environment. We subsequently evaluate three hypotheses that address the limitations of LL optimality models: (1) leaf ageing rates covary strongly with mass-based photosynthetic capacity of mature leaves across species, (2) the predictive power of the optimality model can be enhanced by accounting for both variations of leaf ageing rate and within-canopy variations of light environment and (3) the performance of the optimality model benefits from increased construction cost, especially for canopy-tree leaves. We test the first hypothesis with meta-analysis over 49 species across biomes and the second and third hypotheses with numerical simulations and a functional trait database including well-quantified LL observations for over 100 species, collected in two Panamanian moist lowland forests. Finally, we also investigate the model sensitivity to input leaf functional traits and explore the predicted leaf lifetime-integrated carbon budget.

MATERIAL AND METHODS

Model description

Consistent with the previous optimality approach (Kikuzawa 1991), the central idea of our LL model is to optimise net leaf carbon gain averaged over the entire lifetime of the leaf. To achieve the optimisation, we track the average carbon gain

rate G as a function of leaf age (t ; days), which is calculated as the integration of daily leaf carbon gain ($g(u)$ at day u) over t minus construction cost, divided by t :

$$G(t) = \frac{\int_0^t g(u) du - (CC_{\text{leaf}} + CC_{\text{plant}}) \times \text{LMA}}{t}. \quad (2)$$

CC_{leaf} denotes the leaf-level biochemical cost to build the leaf, which is set to be 1.5 gC gC^{-1} (Villar & Merino 2001, details in Appendix S1). CC_{plant} represents the usually unaccounted for plant-level cost. Because we lack direct measurements of CC_{plant} , we first set it to 0, and then perform a model sensitivity analysis. LMA is regarded as a constant, equal to the LMA of mature leaves because the model treats construction cost as a one-time investment. Differentiating eqn 2 with respect to t and reorganising, we obtain:

$$\frac{dG(t)}{dt} = \frac{g(t) - G(t)}{t}. \quad (3)$$

The optimal LL is defined as the time when $G(t)$ reaches maximum ($dG(t)/dt = 0$), i.e. when $G(t)$ and $g(t)$ are equal. Resolving the optimal LL thus requires estimation of $g(t)$ and $G(t)$.

We adopt a mechanistic photosynthesis model (Farquhar *et al.* 1980) coupled with a stomatal conductance scheme parameterised for tropical evergreen forests (Lin *et al.* 2015) to evaluate the variations in $g(t)$ due to biotic and environmental factors (details in Appendix S1). This photosynthesis model framework is successful to capture carbon assimilation in tropical forests (Wu *et al.* 2017b). The model runs at sub-daily time scale, calculating the diel cycle of carbon assimilation rates driven by changes in light, temperature and vapour pressure deficit. The function $g(t)$ is calculated as the integration of net carbon assimilation rates over the whole day.

Leaf age affects the modelled area-based maximum carboxylation rate (at 25°C , denoted $V_{\text{cmax}25_a}$) and maximum electron transport rate (at 25°C , denoted $J_{\text{max}25_a}$), and thus indirectly influences the realised daily carbon gain. In contrast with previous leaf ageing parameterisation, we also explicitly include leaf maturation process. We assume that $V_{\text{cmax}25_a}$ is zero when leaf age is zero. As leaves develop and mature, $V_{\text{cmax}25}$ increases linearly to a maximum value ($\overline{V_{\text{cmax}25_a}}$) in 2 months, and then declines linearly (top panels in Fig. 1):

$$V_{\text{cmax}25_a}(t) = \overline{V_{\text{cmax}25_a}} \times (1 - t/b). \quad (4)$$

Here, t denotes days since $V_{\text{cmax}25_a}$ begins to decline. b is the age when $V_{\text{cmax}25_a}$ would be zero as in eqn 1, which determines the leaf ageing rate. This linear decline was also adopted in Kikuzawa (1991) and has been corroborated by field observations (Kitajima *et al.* 1997; Wilson *et al.* 2001; Osada *et al.* 2015). In particular, this $V_{\text{cmax}25}$ –age relation with leaf maturation matches well with *in situ* continuous $V_{\text{cmax}25}$ observations in tropical moist forest (Fig. S1). $J_{\text{max}25_a}$, which is parameterised as proportional to $V_{\text{cmax}25_a}$ (Appendix S1), also declines linearly after leaf maturation. Leaf dark respiration rate at 25°C is set to $0.015 \times \overline{V_{\text{cmax}25_a}}$ (Xu *et al.* 2016) and respiration rate remains constant throughout the leaf lifetime, consistent with previous observations for both temperate (Hardwick *et al.*

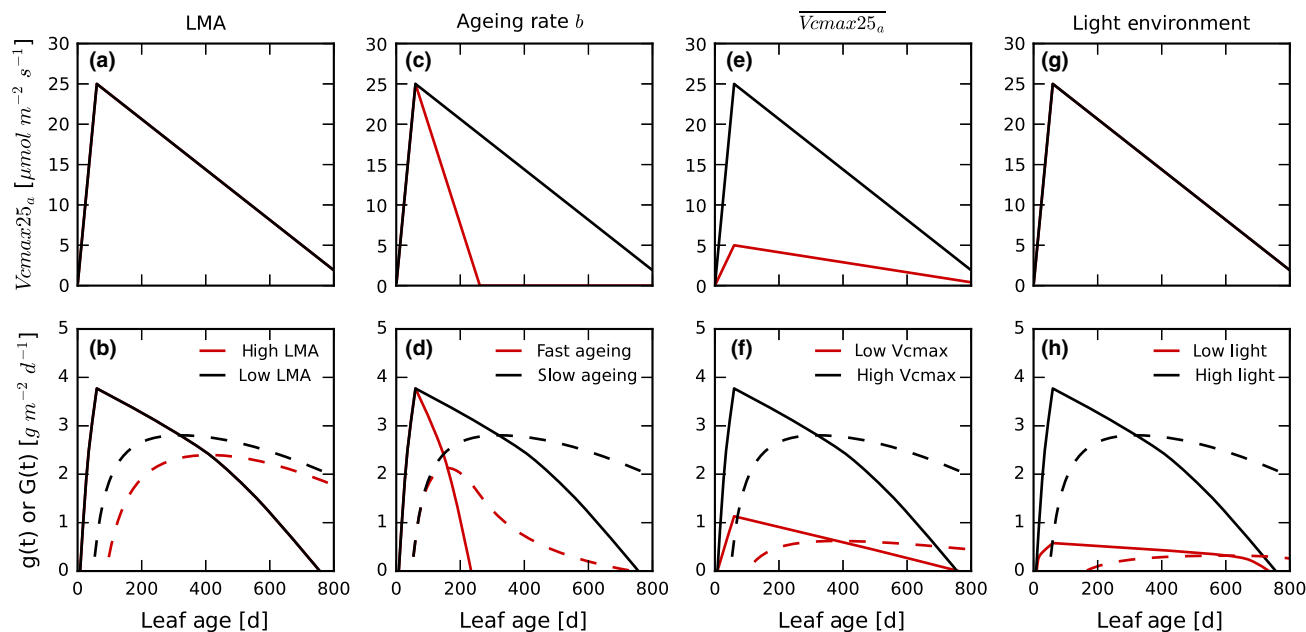


Figure 1 Schematic representation of the partial sensitivity of predicted leaf longevity (LL) to different parameters in our carbon optimality model. Top panels show the ageing rates of area-based maximum carboxylation rate ($V_{cmax25a}$). Bottom panels show instantaneous carbon gain rate ($g(t)$, solid line) and time-averaged carbon gain rate ($G(t)$, dashed line). The leaf age at the intersection of the corresponding solid lines and dashed line represent the optimal LL. In each column, all other model parameters were held the same between black and red lines except for the differences described in the legend. Both top and bottom panels share the same legend in each column. In some panels, red solid line is absent because it exactly overlaps with black solid line.

1968; Xu & Baldocchi 2003) and tropical (Kitajima *et al.* 2002) plants.

The optimal LL cannot be derived analytically in our scheme. Therefore, we track $g(t)$ and $G(t)$ starting from leaf age = 0 and numerically determine the optimal LL by finding the leaf age when $g(t)$ equals $G(t)$ (bottom panels in Fig. 1). Consistent with eqn 1, the predicted LL from our model varies positively with LMA (Fig. 1a and b) and negatively with the ageing rate (Fig. 1c and d). However, the partial sensitivity of predicted LL to changes in $\overline{V_{cmax25a}}$ is relatively small because $G(t)$ and $g(t)$ curves shift in a similar pattern and magnitude, resulting in little change in the intersection of the two curves. In addition to plant functional traits, light environment can strongly affect realised leaf carbon gain and thus influence optimal LL (Fig. 1g and h).

Meta-analysis of photosynthetic capacity decline

We conducted a meta-analysis using data from studies that report both leaf ageing rate and the maximum light-saturated photosynthesis rate during leaf lifetime (Kitajima *et al.* 1997, 2002; Kikuzawa & Lechowicz 2006; Stefanescu 2006; Wu *et al.* 2016, 2017a, G.A. Martins unpublished data). Parameters b , $\overline{V_{cmax25a}}$ and LMA were recorded or estimated for each species (see Appendix S1 for detail). In total, we compiled a dataset including 19 temperate and 30 tropical species (Appendix S2).

We performed regression analysis of the relationship between b and $\overline{V_{cmax25m}}$ mass-based V_{cmax25} , equal to $\overline{V_{cmax25a}}/LMA$. We first used multiple regression to investigate the importance of $\overline{V_{cmax25a}}$ and LMA in determining b .

We then used reduced major-axis regression to estimate the relationship between b and $\overline{V_{cmax25m}}$ because both variables were measured with error (Smith 2009). Results for the tropical species only were used to drive our LL model.

Model input and validation data

We collected leaf functional trait data needed to drive and evaluate our model at two forest sites in Panama. The Fort Sherman/San Lorenzo (FTS, 9°16' N, 79°58' W) site is relatively wet, with annual rainfall averaging 3200 mm and 3–4 months long dry season. The Parque Natural Metropolitano (PNM, 8°59' N, 79°32' W) site is relatively dry, with annual rainfall averaging 1850 mm and 4–5 months long dry season. We obtained hourly measurements of incoming radiation, air temperature and vapour pressure deficit from long-term meteorological station data (http://biogeodb.stri.si.edu/physical_monitoring/).

In the two forests, we censused all leaves on the branches of understory saplings (or the whole sapling if possible) and all leaves on three randomly chosen, fully sun-exposed branches for canopy trees and lianas every month. Two cranes at each site (42 m at PNM and 52 m at FTS) allowed access to the canopy. We used leaves followed from birth to death during 1995 to 2003 to estimate median LL for each species, and included species with six or more LL values in our analysis to avoid observation bias due to small sample size. We measured LMA of fully developed leaves for all species and also estimated light-saturated carbon assimilation rates per area (A_{sat}) by fitting photosynthesis light response curves. These leaf trait data were collected between 1999 and 2002. We then

calculated the corresponding $\overline{V_{cmax25a}}$ by inverting the RuBisCO-limited photosynthesis equation in Farquhar's photosynthesis model (Appendix S1). During the calculation, we assumed that (1) ambient temperature and vapour pressure deficit for A_{sat} measurements are equal to long-term average values at 10:00 AM, (2) leaf temperature for understory leaves is equal to the ambient temperature and (3) leaf temperature for canopy leaves (under direct sunlight) is about 5 °C higher than understory leaves (Rey-Sánchez et al. 2016; Slot & Winter 2017). In total, there are 140 data entries (102 for canopy leaves, 38 for understory leaves) from 105 species in our study (Appendix S3). Most of the data (102 of 140) are for evergreen species based on local expertise.

Numerical experiments

We conducted three sets of simulations (*S1–S3*). In set *S1*, we used the same b value for all leaves, calculated from the average $\overline{V_{cmax25m}}$ across all leaves using the relationship derived in our meta-analysis. All leaves receive canopy-level light. In set *S2*, we set different b values across leaves, which were calculated from the observed $\overline{V_{cmax25m}}$ for each leaf. All leaves receive canopy-level light. Set *S3* is the same as *S2* except that canopy leaves receive canopy-level light and understory leaves receive understory-level light. Simulation *S3* serves to evaluate the performance of optimality principle to explain LL variations, while the comparison of *S1–S3* shows the importance of leaf ageing rate and within-canopy light gradient.

All simulation sets were driven by the observed LMA, $\overline{V_{cmax25a}}$ and multi-year average diel cycles of meteorological forcing (Fig. S2). Because the optimal LL under average environmental conditions is our major interest, climatic seasonality was not included in our analysis for simplicity. Light level was derived from the observed incoming radiation and a multi-layer canopy radiative transfer model (Appendix S1). In the radiative transfer model, the total forest LAI is set as 6 according to field observations. Light received by the top 1 LAI was used as canopy-level light and light received by the bottom 1 LAI was used as understory-level light (Fig. S2). To compare the predicted LL with the observations, the predicted LL was subtracted by the time to reach maturity in our model (2 months) because the leaf age was treated as zero for fully expanded leaves in observations. Correlation and reduced major-axis regression analysis was performed between the predicted LL and the observed LMA, $\overline{V_{cmax25a}}$ and LL. All variables were log transformed before statistical analysis.

In all three simulations, CC_{plant} was set to zero. To investigate the model sensitivity to plant-level construction cost, we performed additional simulations, following the assumptions in simulation set *S3*. Earlier studies estimated CC_{plant} as between 0.1 and 1.1 time of CC_{leaf} (Kikuzawa & Ackerly 1999). Thus, we gradually increased CC_{plant} from 0 to 2 times of CC_{leaf} . We examined the changes in the correlation, regression slope and normalised root mean square error (NRMSE) between predicted LL and the observed values.

Finally, we investigated the model sensitivity to changes in the values of LMA and $\overline{V_{cmax25a}}$. We calculated the predicted LL and the associated optimal average lifetime carbon gain rate (maximum $G(t)$ in eqn 2) for different combinations

of LMA and $\overline{V_{cmax25a}}$ within the observed range (10–250 g m⁻² for LMA and 5–150 μmol m⁻² s⁻¹ for $\overline{V_{cmax25a}}$). Furthermore, we calculated the total leaf lifetime carbon gain per leaf biomass if leaves senesce at the predicted LL. This value measures leaf lifetime net carbon gain (LCG), which has been proposed to either be independent from LL (Mediavilla & Escudero 2003; Kikuzawa & Lechowicz 2006) or to increase with LL (Falster et al. 2012).

We used Python version 2.7 (Python Software Foundation, <http://www.python.org>) for all our analyses. The code for our model and experiments can be found in Appendix S4.

RESULTS

Leaf ageing rate

Our meta-analysis shows that the parameter b (the inverse of leaf ageing rate) varies by two orders of magnitude (Fig. 2), ranging from 36 to 4509 days. Over all species, b is negatively correlated with mass-based photosynthetic capacity, $\overline{V_{cmax25m}}$ ($r = -0.83$, $P \ll 0.001$). Because $\overline{V_{cmax25m}}$ depends on both $\overline{V_{cmax25a}}$ and LMA, we further checked the relation between b and these two functional traits separately (Fig. S3). Our results show that b is negatively correlated with $\overline{V_{cmax25a}}$ ($r = -0.43$, $P = 0.007$) and positively correlated with LMA ($r = 0.73$, $P \ll 0.001$). Meanwhile there is no significant correlation between LMA and $\overline{V_{cmax25a}}$ ($r = -0.08$, $P = 0.65$). Multiple regression analysis also suggests that both functional traits should be incorporated to better infer b (Table S1).

The correlation between b and $\overline{V_{cmax25m}}$ is preserved when we consider only tropical species ($r = -0.73$, $P \ll 0.001$). The slope and intercept values from reduced major-axis regression

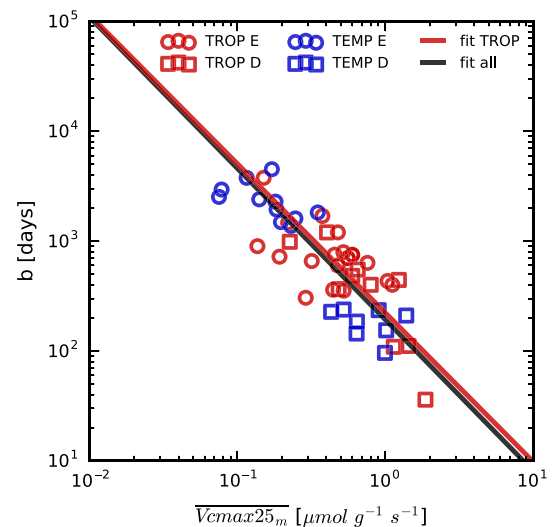


Figure 2 The coordination of the parameter b that represents leaf ageing rate (see eqn 4 for details) with mass-based photosynthetic capacity in log-space from meta-analysis. Blue and red points represent temperate and tropical species, respectively. Squares and circles represent deciduous and evergreen species, respectively. Black and red lines represent reduced major-axis regression relationships for all species and tropical species only respectively.

are very similar between all data (−1.38, 2.29) and tropical data (−1.36, 2.35). In general, deciduous species have higher $\overline{V_{cmax25_m}}$ and lower b values while evergreen species show the opposite (Fig. 2). This leaf habit separation is more prominent among temperate species than tropical species.

Observed and simulated variations of LL

In situ observations of LL range from 35 to 1855 days. Over all leaves, the observed LL is not correlated with LMA ($r = -0.002$, $P = 0.98$), but is negatively correlated with $\overline{V_{cmax25_a}}$ ($r = -0.44$, $P \ll 0.001$). However, there is large within-canopy variation in leaf functional traits. After separating the data into canopy leaves and understory leaves, the observed LL is positively correlated with LMA but is not correlated with $\overline{V_{cmax25_a}}$ within each forest stratum (Fig. 3a–b and Table 1).

In simulation *S1*, the model underestimated the range of LL (*c.* 150 vs. *c.* 1500 days) by an order of magnitude, biasing the relationship between the predicted LL and the observed functional traits (Fig. 3c–e). We obtained a better prediction

of LL in simulation set *S2* because of the inclusion of variation in parameter b . The regression slope between the simulated and the observed LL increased from *c.* 0.12 in simulation *S1* to 0.7–0.8 in simulation *S2* (cf. Fig. 3e and h). As a result, the slopes of the predicted LL against LMA and $\overline{V_{cmax25_a}}$ became much closer to the observed values (Table 1, Fig. 3f and g).

Inclusion of the realistic understory light levels in simulation set *S3* increased the predicted LL for understory leaves (Fig. 3k). The regression slopes between the predicted and the observed LL for all the leaves became very close to 1 (1.03). However, the slopes within-canopy and understory subgroups were still biased low. In this simulation, the predicted LL is not correlated with LMA over all the leaves, which is consistent with the observations (cf. Fig. 3a and i) and the slope of the predicted LL– $\overline{V_{cmax25_a}}$ relationship (−1.20) is similar to the value derived from observations (−1.13; cf. Fig. 3b and j). This fundamental pattern persists when we include only evergreen species in our analysis (Fig. S4).

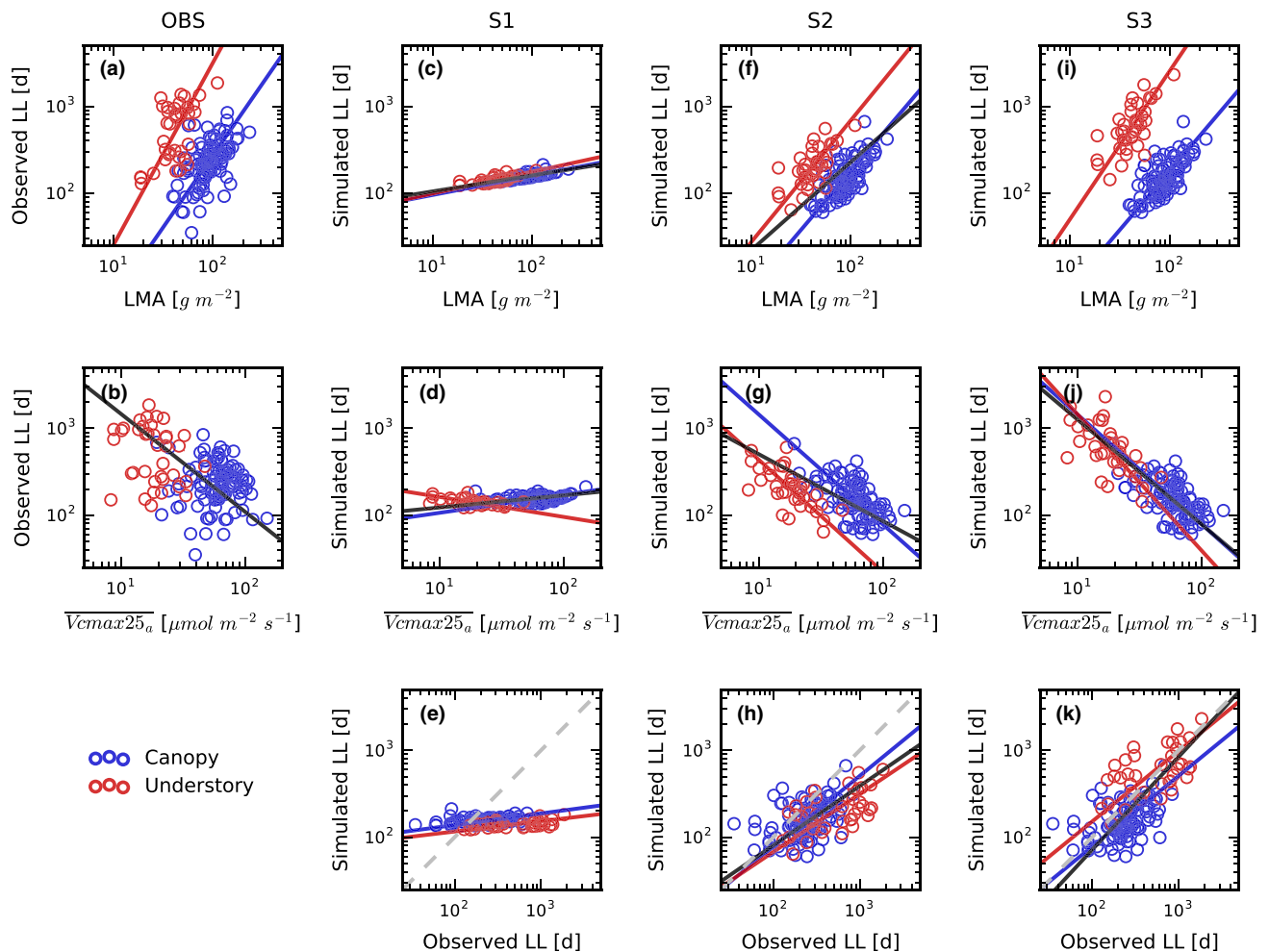


Figure 3 The relation between the observed leaf longevity (LL) and plant functional traits in our Panamanian trait data set (a–b). The relation between the predicted LL with the two input functional traits and the observed LL for three different model set ups (c–k, see Material and Methods section for details). Each dot represents a species. In each panel, a line is drawn if there is a significant correlation ($P < 0.05$) for canopy leaves (blue), understory leaves (red) or all the leaves (black). Statistical analysis results can be found in Table 1.

Table 1 Statistical analysis for the leaf longevity (LL) results of Fig. 3.

	OBS LL	LL in S1	LL in S2	LL in S3
vs. LMA (canopy)	1.66 (1.37, 1.93) $r = \mathbf{0.53}^*$	0.22 (0.20, 0.24) $r = \mathbf{0.85}^*$	1.35 (1.16, 1.53) $r = \mathbf{0.71}^*$	1.35 (1.16, 1.53) $r = \mathbf{0.71}^*$
vs. LMA (understory)	2.10 (1.51, 2.69) $r = \mathbf{0.55}^*$	0.25 (0.20, 0.30) $r = \mathbf{0.77}^*$	1.40 (1.05, 1.75) $r = \mathbf{0.67}^*$	1.70 (1.29, 2.11) $r = \mathbf{0.70}^*$
vs. LMA (all)	$r = 0.00$	0.18 (0.17, 0.20) $r = \mathbf{0.84}^*$	1.01 (0.85, 1.17) $r = \mathbf{0.32}^*$	$r = -0.18$
vs. $\overline{Vcmax25_a}$ (canopy)	$r = -0.04$	0.21 (0.17, 0.25) $r = \mathbf{0.26}$	-1.27 (-1.47, -1.06) $r = \mathbf{-0.58}^*$	-1.27 (-1.47, -1.06) $r = \mathbf{-0.58}^*$
vs. $\overline{Vcmax25_a}$ (understory)	$r = -0.21$	-0.23 (-0.30, -0.16) $r = \mathbf{-0.47}$	-1.29 (-1.62, -0.96) $r = \mathbf{-0.67}^*$	-1.57 (-1.98, -1.15) $r = \mathbf{-0.63}$
vs. $\overline{Vcmax25_a}$ (all)	-1.13 (-1.30, -0.96) $r = \mathbf{-0.44}^*$	0.14 (0.12, 0.16) $r = \mathbf{0.37}^*$	-0.77 (-0.88, -0.66) $r = \mathbf{-0.54}^*$	-1.20 (-1.32, -1.09) $r = \mathbf{-0.84}^*$
vs. OBS LL (canopy)	N/A	0.13 (0.11, 0.16) $r = \mathbf{0.32}^*$	0.81 (0.67, 0.96) $r = \mathbf{0.45}^*$	0.81 (0.67, 0.96) $r = \mathbf{0.45}^*$
vs. OBS LL (understory)	N/A	0.12 (0.08, 0.15) $r = \mathbf{0.48}$	0.67 (0.48, 0.85) $r = \mathbf{0.56}^*$	0.81 (0.59, 1.03) $r = \mathbf{0.58}^*$
vs. OBS LL (all)	N/A	$r = 0.08$	0.68 (0.59, 0.78) $r = \mathbf{0.53}^*$	1.07 (0.93, 1.21) $r = \mathbf{0.66}^*$

Each cell records the slope from reduced major axis regression (95% CI in parentheses) and Pearson's r . Bolded values indicate $P < 0.01$ and *indicates $P < 0.001$. Regression results are only displayed when correlation $P < 0.01$. All the variables were log-transformed before analysis.

Model sensitivity to parameters

The performance of our optimality model overall is not very sensitive to parameter CC_{plant} (Fig. 4) because changes in construction cost only mildly influence leaf lifetime carbon economy (Fig. 1b). When $CC_{\text{plant}}/CC_{\text{leaf}}$ increased from 0 to 2, the correlation between the observed and simulated LL decreased a little while regression slope slowly deviated away from 1. Meanwhile, the model bias measured by NRMSE decreased first and then increased. Canopy and understory leaves showed different patterns. Model performance was best when $CC_{\text{plant}}/CC_{\text{leaf}}$ was *c.* 0.8 for canopy leaves, but when the ratio was 0 for understory leaves.

Figure 5 presents the model sensitivity to the two input functional traits for canopy and understory leaves. The predicted LL is very sensitive to LMA while it is only sensitive to $\overline{Vcmax25_a}$ when LMA is large (Fig. 5a and b). In contrast, the predicted area-based optimal net carbon gain rate ($G(t)$) is mostly controlled by $\overline{Vcmax25_a}$ (Fig. 5c and d). For canopy leaves, $G(t)$ reaches a maximum when $\overline{Vcmax25_a}$ is around 50–100 $\mu\text{mol m}^{-2} \text{s}^{-1}$. For understory leaves, $G(t)$ is only positive when $\overline{Vcmax25_a}$ is lower than 20 $\mu\text{mol m}^{-2} \text{s}^{-1}$ and monotonically decreases as $\overline{Vcmax25_a}$ increases. Finally, LCG is relatively insensitive to LMA and decreases with increasing $\overline{Vcmax25_a}$ (Fig. 5e and f). Under canopy light, leaves within the range of $\overline{Vcmax25_a}$ observed in tropical forests (20–100 $\mu\text{mol m}^{-2} \text{s}^{-1}$) are predicted to achieve LCG equivalent to 4–12 times of its leaf biomass. Under understory light, leaves with very low $\overline{Vcmax25_a}$ can still achieve high LCG because their LL can be very long (Fig. 5b).

DISCUSSION

Coordination between leaf ageing rate and mass-based photosynthetic capacity

Our meta-analysis supports the hypothesis that leaf ageing rate (the inverse of b) covaries with area-based maximum

carboxylation rate ($\overline{Vcmax25_a}$) and leaf structure (LMA) and thus can be best inferred from mass-based $\overline{Vcmax25_m}$ (Fig. 2, Table S1). This relation may ultimately be driven by both ecological coordination with plant growth strategy and plant defence against environmental stresses. The decline in photosynthetic capacity can be caused by the reduction in either leaf nitrogen concentration or nitrogen use efficiency (Kitajima *et al.* 1997; Mediavilla & Escudero 2003). First, the reduction in nitrogen concentration is possibly because self-shading can occur during shoot extension (Field 1983) and plants redistribute nitrogen from old leaves to new leaves (Ackerly 1999). Leaves with high $\overline{Vcmax25_m}$ usually belong to fast-growing and shade-intolerant species, which could benefit from fast nitrogen resorption and high photosynthetic decline rate. In contrast, species with low $\overline{Vcmax25_m}$ are less nitrogen demanding and more tolerant to shading. Therefore, it is not necessary for those plants to resorb nitrogen rapidly. However, leaf ageing rates of most tropical species in our meta-analysis are unlikely due to self-shading because leaf light environment did not change much during repeated measurements (Kitajima *et al.* 1997; Stefanescu 2006). Second, the reduction in nitrogen use efficiency can be caused by accumulated damage of photosynthetic enzymes or reduced mesophyll conductance (Flexas *et al.* 2008) due to multiple environmental stressors (Xu & Baldocchi 2003; Monaghan *et al.* 2009). Leaves with high $\overline{Vcmax25_m}$ would have less protection per unit photosynthetic machinery and show a faster ageing rate.

In our analysis, the coordination between leaf ageing rate and $\overline{Vcmax25_m}$ is conserved across species, leaf habit types (deciduous vs. evergreen) and biomes. However, it is noteworthy that the correlation across biomes is stronger than the correlation within the same biome (Fig. 2). For example, temperate deciduous species show relatively small variation in leaf ageing rates. This is possibly because of an adaptation to the strong seasonality of radiation and photoperiod in temperate regions (Bauerle *et al.* 2012). Compilation of more data is

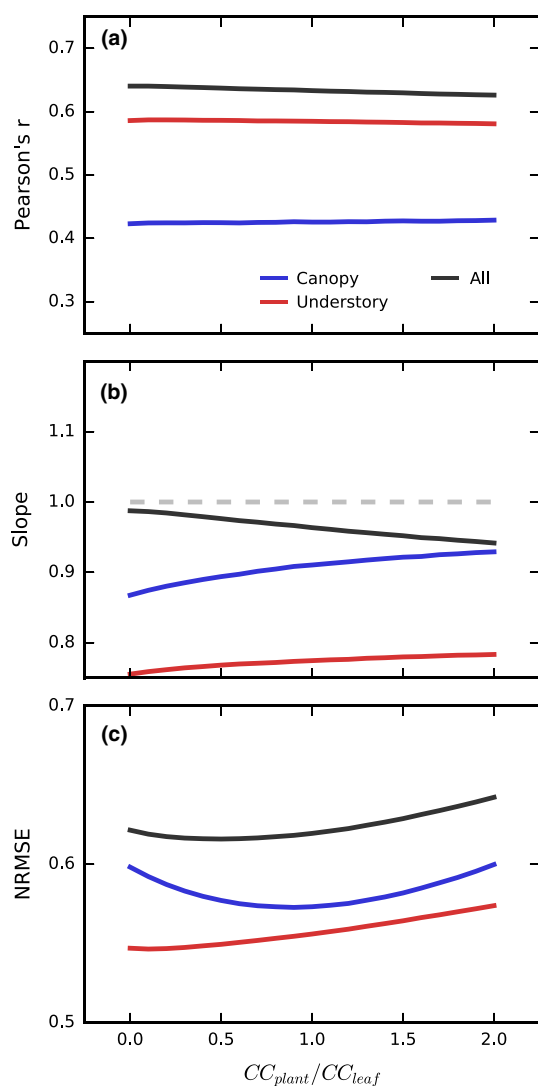


Figure 4 Model sensitivity to changes in plant-level construction cost (CC_{plant}). The model performance was quantified by (a) the correlation between the predicted and observed leaf longevity, (b) the slope from reduced major axis regression and (c) normalised root mean square error (NRMSE). Results for canopy leaves (blue), understory leaves (red) and all leaves (black) are shown.

necessary to advance our understanding of the leaf ageing process in temperate forests.

In our carbon optimality model, the coordination between leaf ageing rate and $\overline{V_{\text{cmax}25_m}}$ is critical to model performance (Fig. 3). The incorporation of leaf-specific b values estimated from the coordination significantly reduced the bias between the predicted and observed LL (cf. $S1$ and $S2$ in Table 1).

Within-canopy variation in LL and the leaf economics spectrum (LES)

LL varies widely between conspecific sun and shade leaves (32 species in total) in our tropical data set (Fig. S5). Regression analysis shows that there is no strong trait covariance when all leaves were grouped together (Fig. 3a), which indicates

that an LES derived from global scale (Wright *et al.* 2004) cannot be blithely applied at local scale. Trait covariance is recovered when we group leaves sharing similar microenvironments (i.e. canopy and understory leaves), suggesting that the LES slope and intercept can be influenced by environmental factors (Wright *et al.* 2005).

Our analysis demonstrates that the within-canopy variations of LL and LES can be accounted for in our carbon optimality model. Under simulation $S3$, the predicted LL is higher for understory leaves with a given LMA compared with canopy leaves. The predicted LL-LMA slope for low light-level understory is also larger than the slope for high light-level canopy leaves (Table 1), which is consistent with our data set and other analyses (Wright *et al.* 2005). The model can capture this within-canopy variation for two reasons. First, although understory leaves have lower $\overline{V_{\text{cmax}25_a}}$ and LMA compared with canopy leaves (Fig. S5), they generally have low $\overline{V_{\text{cmax}25_m}}$ and thus have low leaf ageing rates in our model. This is consistent with the idea that shade-tolerant understory leaves should invest more resources to build tough leaves in tropical forests (Kitajima *et al.* 2012). Therefore, the incorporation of leaf-specific b values helps the model to partly capture within-canopy variation (cf. $S2$ and $S1$ in Fig. 3). Second, understory leaves achieve lower carbon gain due to strong light limitation (cf. Fig. 5c and d). To reach carbon optimality in our model, the understory leaves need to survive longer (cf. $S3$ and $S2$ in Fig. 3). These results support our second hypothesis that both variations of leaf ageing rate and light environment are critical to predicting within-canopy variations of LL.

The remaining difference between the simulated and observed LL reflects possible limitations in our LL optimality model. First, leaf morphological, structural and nutrient traits that are not included in the optimality model might modify realised LL (Wright & Westoby 2003; Kitajima *et al.* 2012). However, further quantitative analysis shows that the residuals are not correlated with those traits (Fig. S6). Second, our leaf-level carbon optimisation criterion is most appropriate when the growth environment does not change significantly throughout leaf lifetime (Kikuzawa 1991). However, leaf light environment can decrease radically due to self-shading, especially for fast-growing plants. In this case, the optimisation should operate at canopy scale by keeping the old shaded leaves until their daily carbon gain becomes zero due to self-shading (Ackerly 1999). This change in optimisation criterion could lead to longer LL. Third, we assumed young leaves needed 2 months to expand and mature based on observations of two Amazonian species (Fig. S1). Some tropical species expand their leaves in as little as 2 weeks, possibly to avoid herbivore damage (Coley & Barone 1996). Reducing the period of leaf maturation in our model would increase the simulated LL values. Fourth, construction cost might not be a constant for different leaves. For example, canopy leaves require more carbon for supporting tissues, nutrient transportation and photoprotection (Steyn *et al.* 2002) compared with understory leaves. Resorption of carbon and other nutrient during leaf senescence (Wright & Westoby 2003; Vergutz *et al.* 2012) and its associated energetic cost might also vary among canopy and understory leaves and thus change the net

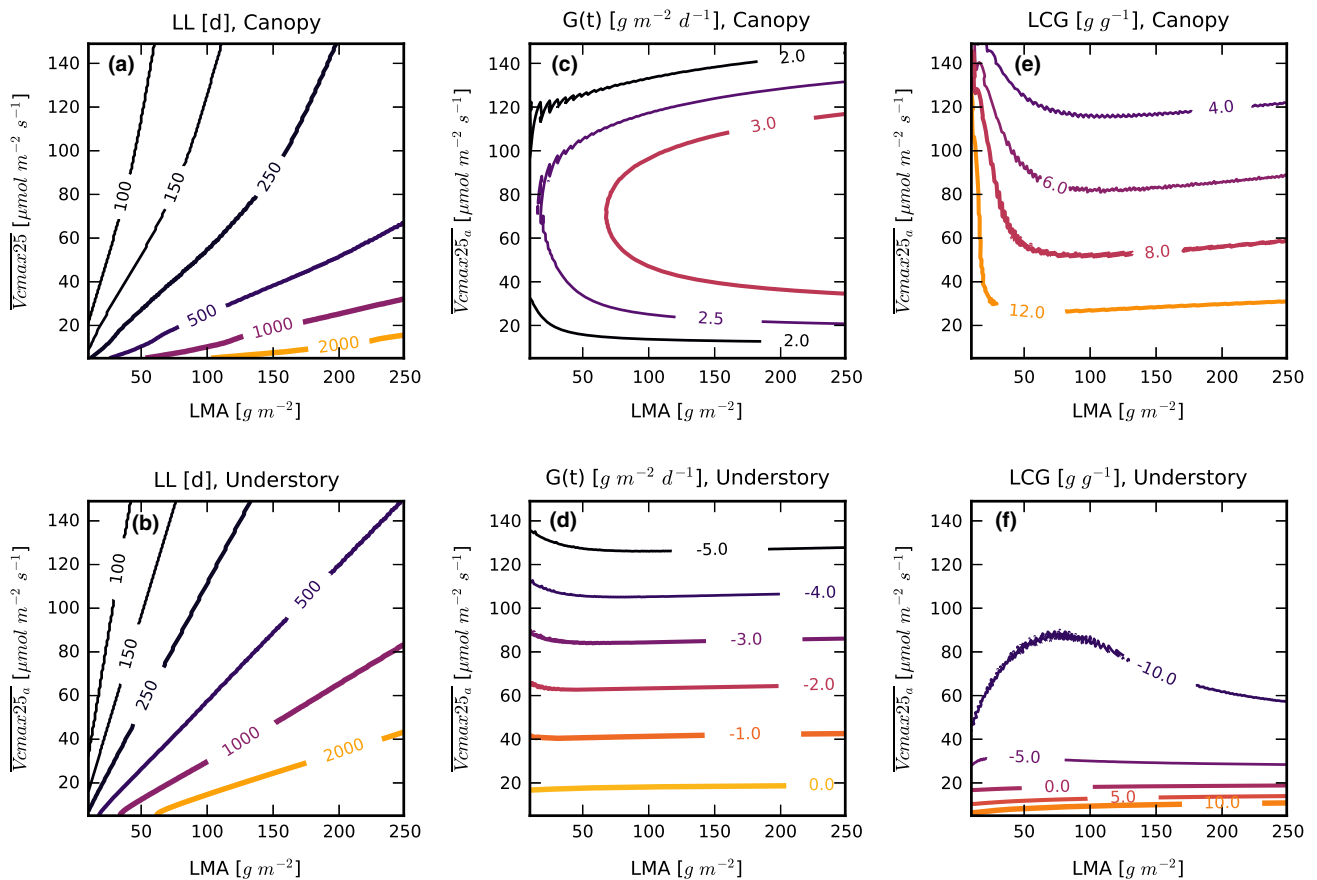


Figure 5 Contour plots for the predicted leaf longevity (LL, a–b), leaf lifetime average carbon gain rate ($G(t)$, c–d) and mass-based leaf lifetime carbon gain (LCG, e–f) for different combinations of input plant functional traits. The top panels show results with canopy light and bottom panels show the results with understory light. The model setup is the same as S3 and CC_{plant} was set to be zero.

leaf construction cost. Our sensitivity test shows that the regression slope becomes closer to 1 and NRMSE decreases for canopy leaves under higher CC_{plant} , supporting our third hypothesis that the model performance benefits from increased construction cost for canopy-tree leaves (Fig. 4). However, the performance improvement is marginal, especially measured from the correlation between the predicted and observed LL values.

Optimal leaf lifetime carbon gain

The central feature of the carbon optimality model is to regard LL as a mechanism to optimise leaf lifetime carbon gain. In our approach, the optimised area-based net lifetime carbon gain rate ($G(t)$) is mainly controlled by $\overline{Vcmax25_a}$. Interestingly, in our tropical data set, the average $\overline{Vcmax25_a}$ is $19.7 \mu\text{mol m}^{-2} \text{s}^{-1}$ for understory leaves and $63.2 \mu\text{mol m}^{-2} \text{s}^{-1}$ for canopy leaves, which are very close to the $\overline{Vcmax25_a}$ values that allow high $G(t)$ in our model predictions (Fig. 5c and d). This result suggests that plants can actively adjust leaf biochemical properties to reach optimal carbon gain in accordance with light availability (Lloyd *et al.* 2010).

Previous studies have reported that leaf lifetime return (equivalent to LCG + CC in our model) is independent from LL (Mediavilla & Escudero 2003; Kikuzawa & Lechowicz

2006). In our approach, the predicted leaf lifetime return increases with LL because the average carbon gain rate is not exactly proportional to the inverse of LL (Fig. S7). Our results agree with another modelling study which focused on a smaller data set from an Australian forest (Falster *et al.* 2012). However, if leaf lifetime return increases with LL, why are there still many species with short LL? One explanation is that the value of carbon gain might be discounted with time (Westoby *et al.* 2000). The benefit of long-lived leaves can only be realised when the leaves can actually live to their optimal age. Various environmental stresses, including herbivory and disturbances such as wind storms, can kill leaves before their optimal age. The potential damage can be reduced for leaves with short LL. On the other hand, the light level could decrease significantly due to leaf over-topping especially for early-successional species colonising forest gaps. Short LL allows these plants to quickly redistribute nitrogen within individual canopy and achieve better whole-plant nitrogen use efficiency (Field & Mooney 1983).

There are few estimates for lifetime net carbon return rate of leaves in tropical rainforests. Williams *et al.* (1989) reported that leaf lifetime carbon gain can exceed 10 for canopy leaves for the genus *Piper*. Another way to estimate whole-canopy leaf lifetime return is to calculate the ratio of gross primary production minus leaf respiration (carbon gain)

over net primary production allocated to leaves (normalisation by leaf mass). This ratio is about 7 in Amazonian rain forests (data from Malhi *et al.* 2011), which falls in our predicted range (5–20).

CONCLUSION

The leaf life cycle has been recognised as critical for understanding tropical seasonality and carbon dynamics (Kim *et al.* 2012; Restrepo-Coupe *et al.* 2016; Wu *et al.* 2016). Our results show that LL, a key metric of the leaf life cycle, can be quantitatively predicted with a leaf-level carbon optimality model if realistic rates of leaf ageing and micro-environment are incorporated. Our model may be used to help to reduce uncertainties in projected vegetation dynamics in tropical forests (Huntingford *et al.* 2013). Moreover, this model can be extended to consider the leaf-level economy of other nutrients (Falster *et al.* 2012) and has the potential to capture the adaptive responses of LL to environmental changes such as warming (Kikuzawa *et al.* 2013). It will be of great interest to investigate whether the carbon optimality model can capture the changes in LL and leaf economics spectrum across various environmental gradients (Wright *et al.* 2005) as well as under CO₂ fertilisation and nutrient addition (Craine & Reich 2001). It is also noteworthy that the physiological pathway that allows the plants to shed leaves at optimal carbon gain is still not clear. Meanwhile, a large portion of the variation in LL is not explained by the carbon optimality model or other functional traits. These remaining knowledge gaps invite further investigations in the future.

ACKNOWLEDGEMENT

We thank Colin Prentice and two anonymous reviewers for their help to improve the manuscript. DM gratefully acknowledges support from US Department of Energy Terrestrial Ecosystem Science award DE-SC0014363. Leaf demography censuses in Panama were supported by a grant from the Andrew W. Mellon Foundation to SJW. SRS, JW and LPA acknowledge supports from NSF PIRE (no. 0730305) and NASA Terra-Aqua Science program (NNX11AH24G). JW was supported by DOE (BER) NGEE-Tropics projects at Brookhaven National Laboratory.

AUTHORSHIP

XX and DM designed the research. XX performed the analysis. SJW, KK, JW, LPA, GAM and SRS provided field data for analysis. JW provided critical analytical tools. XX drafted the paper and all authors contributed to writing of the manuscript.

CONFLICT OF INTEREST

The authors declare no conflict of interest.

DATA ACCESSIBILITY STATEMENT

All data and code used in the analysis are freely available online.

REFERENCES

- Ackerly, D. (1999). Self-shading, carbon gain and leaf dynamics: a test of alternative optimality models. *Oecologia*, 119, 300–310.
- Bauerle, W.L., Oren, R., Way, D.A., Qian, S.S., Stoy, P.C., Thornton, P.E. *et al.* (2012). Photoperiodic regulation of the seasonal pattern of photosynthetic capacity and the implications for carbon cycling. *Proc. Natl Acad. Sci. USA*, 109, 8612–8617.
- Blonder, B., Violle, C., Bentley, L.P. & Enquist, B.J. (2011). Venation networks and the origin of the leaf economics spectrum. *Ecol. Lett.*, 14, 91–100.
- Chabot, B.F. & Hicks, D.J. (1982). The ecology of leaf life spans. *Annu. Rev. Ecol. Syst.*, 13, 229–259.
- Coley, P.D. & Barone, J.A. (1996). Herbivory and plant defenses in tropical forests. *Annu. Rev. Ecol. Syst.*, 27, 305–335.
- Craine, J.M. & Reich, P.B. (2001). Elevated CO₂ and nitrogen supply alter leaf longevity of grassland species. *New Phytol.*, 150, 397–403.
- Falster, D.S., Reich, P.B., Ellsworth, D.S., Wright, I.J., Westoby, M., Oleksyn, J. *et al.* (2012). Lifetime return on investment increases with leaf lifespan among 10 Australian woodland species. *New Phytol.*, 193, 409–419.
- Farquhar, G.D., Caemmerer, S.V. & Berry, J.A. (1980). A biochemical model of photosynthetic CO₂ assimilation in leaves of C-3 species. *Planta*, 149, 78–90.
- Field, C. (1983). Allocating leaf nitrogen for the maximization of carbon gain: leaf age as a control on the allocation program. *Oecologia*, 56, 341–347.
- Field, C. & Mooney, H. (1983). Leaf age and seasonal effects on light, water, and nitrogen use efficiency in a California shrub. *Oecologia*, 56, 348–355.
- Flexas, J., Ribas-Carbó, M., Diaz-Espejo, A., Galmés, J. & Medrano, H. (2008). Mesophyll conductance to CO₂: current knowledge and future prospects. *Plant Cell Environ.*, 31, 602–621.
- Hardwick, K., Wood, M. & Woolhouse, H.W. (1968). Photosynthesis and respiration in relation to leaf age in *Perilla frutescens* (L.) Britt. *New Phytol.*, 67, 79–86.
- Huntingford, C., Zelazowski, P., Galbraith, D., Mercado, L.M., Sitch, S., Fisher, R. *et al.* (2013). Simulated resilience of tropical rainforests to CO₂-induced climate change. *Nat. Geosci.*, 6, 268–273.
- Kikuzawa, K. (1991). A cost-benefit analysis of leaf habit and leaf longevity of trees and their geographical pattern. *Am. Nat.*, 138, 1250–1263.
- Kikuzawa, K. & Ackerly, D. (1999). Significance of leaf longevity in plants. *Plant Species Biol.*, 14, 39–45.
- Kikuzawa, K. & Lechowicz, M., Associate Editor: Volker, G. & Editor: Donald, L.D. (2006). Toward synthesis of relationships among leaf longevity, instantaneous photosynthetic rate, lifetime leaf carbon gain, and the gross primary production of forests. *Am. Nat.*, 168, 373–383.
- Kikuzawa, K., Shirakawa, H., Suzuki, M. & Umeki, K. (2004). Mean labor time of a leaf. *Ecol. Res.*, 19, 365–374.
- Kikuzawa, K., Onoda, Y., Wright, I.J. & Reich, P.B. (2013). Mechanisms underlying global temperature-related patterns in leaf longevity. *Glob. Ecol. Biogeogr.*, 22, 982–993.
- Kim, Y., Knox, R.G., Longo, M., Medvigy, D., Hutryra, L.R., Pyle, E.H. *et al.* (2012). Seasonal carbon dynamics and water fluxes in an Amazon rainforest. *Glob. Chang. Biol.*, 18, 1322–1334.
- Kitajima, K., Mulkey, S. & Wright, S. (1997). Decline of photosynthetic capacity with leaf age in relation to leaf longevities for five tropical canopy tree species. *Am. J. Bot.*, 84, 702.
- Kitajima, K., Mulkey, S.S., Samaniego, M. & Joseph Wright, S. (2002). Decline of photosynthetic capacity with leaf age and position in two tropical pioneer tree species. *Am. J. Bot.*, 89, 1925–1932.
- Kitajima, K., Llorens, A.-M., Stefanescu, C., Timchenko, M.V., Lucas, P.W. & Wright, S.J. (2012). How cellulose-based leaf toughness and lamina density contribute to long leaf lifespans of shade-tolerant species. *New Phytol.*, 195, 640–652.

- Kitajima, K., Cordero, R.A. & Wright, S.J. (2013). Leaf life span spectrum of tropical woody seedlings: effects of light and ontogeny and consequences for survival. *Ann. Bot.*, 112, 685–699.
- Lin, Y.-S., Medlyn, B.E., Duursma, R.A., Prentice, I.C., Wang, H., Baig, S. *et al.* (2015). Optimal stomatal behaviour around the world. *Nat. Clim. Chang.*, 5, 459–464.
- Lloyd, J., Patiño, S., Paiva, R.Q., Nardoto, G.B., Quesada, C.A., Santos, A.J.B. *et al.* (2010). Optimisation of photosynthetic carbon gain and within-canopy gradients of associated foliar traits for Amazon forest trees. *Biogeosciences*, 7, 1833–1859.
- Lusk, C.H., Reich, P.B., Montgomery, R.A., Ackerly, D.D. & Cavender-Bares, J. (2008). Why are evergreen leaves so contrary about shade?. *Trends Ecol. Evol.*, 23, 299–303.
- Malhi, Y., Doughty, C. & Galbraith, D. (2011). The allocation of ecosystem net primary productivity in tropical forests. *Philos. Trans. R. Soc. B-Biol. Sci.*, 366, 3225–3245.
- McMurtrie, R.E. & Dewar, R.C. (2011). Leaf-trait variation explained by the hypothesis that plants maximize their canopy carbon export over the lifespan of leaves. *Tree Physiol.*, 31, 1007–1023.
- Mediavilla, S. & Escudero, A. (2003). Photosynthetic capacity, integrated over the lifetime of a leaf, is predicted to be independent of leaf longevity in some tree species. *New Phytol.*, 159, 203–211.
- Monaghan, P., Metcalfe, N.B. & Torres, R. (2009). Oxidative stress as a mediator of life history trade-offs: mechanisms, measurements and interpretation. *Ecol. Lett.*, 12, 75–92.
- Osada, N., Oikawa, S. & Kitajima, K. (2015). Implications of life span variation within a leaf cohort for evaluation of the optimal timing of leaf shedding. *Funct. Ecol.*, 29, 308–314.
- Reich, P.B., Uhl, C., Walters, M.B. & Ellsworth, D.S. (1991). Leaf lifespan as a determinant of leaf structure and function among 23 amazonian tree species. *Oecologia*, 86, 16–24.
- Restrepo-Coupe, N., Levine, N.M., Christoffersen, B.O., Albert, L.P., Wu, J., Costa, M.H. *et al.* (2016). Do dynamic global vegetation models capture the seasonality of carbon fluxes in the Amazon basin? A data-model intercomparison. *Glob. Chang. Biol.*, 23, 191–208.
- Rey-Sánchez, A., Slot, M., Posada, J. & Kitajima, K. (2016). Spatial and seasonal variation in leaf temperature within the canopy of a tropical forest. *Clim. Res.*, 71, 75–89.
- Russo, S.E. & Kitajima, K. (2016). The ecophysiology of leaf lifespan in tropical forests: adaptive and plastic responses to environmental heterogeneity. In: *Tropical Tree Physiology: Adaptations and Responses in a Changing Environment*. (eds Goldstein, G., Santiago, L.S.). Springer International Publishing, Cham, pp. 357–383.
- Slot, M. & Winter, K. (2017). In situ temperature response of photosynthesis of 42 tree and liana species in the canopy of two Panamanian lowland tropical forests with contrasting rainfall regimes. *New Phytol.*, 214, 1103–1117.
- Smith, R.J. (2009). Use and misuse of the reduced major axis for line-fitting. *Am. J. Phys. Anthropol.*, 140, 476–486.
- Stefanescu, C. (2006). Cost-benefit theory of leaf lifespan in seedlings of tropical tree species (*Master Dissertation*). Retrieved from University of Florida (<http://ufdc.ufl.edu/UFE0015764/00001>).
- Steyn, W.J., Wand, S.J.E., Holcroft, D.M. & Jacobs, G. (2002). Anthocyanins in vegetative tissues: a proposed unified function in photoprotection. *New Phytol.*, 155, 349–361.
- Vergutz, L., Manzoni, S., Porporato, A., Novais, R.F. & Jackson, R.B. (2012). Global resorption efficiencies and concentrations of carbon and nutrients in leaves of terrestrial plants. *Ecol. Monogr.*, 82, 205–220.
- Villar, R. & Merino, J. (2001). Comparison of leaf construction costs in woody species with differing leaf life-spans in contrasting ecosystems. *New Phytol.*, 151, 213–226.
- Westoby, M., Warton, D. & Reich, P.B. (2000). The time value of leaf area. *Am. Nat.*, 155, 649–656.
- Williams, K., Field, C.B. & Mooney, H.A. (1989). Relationships among leaf construction cost, leaf longevity, and light environment in rain-forest plants of the genus piper. *Am. Nat.*, 133, 198–211.
- Wilson, K.B., Baldocchi, D.D. & Hanson, P.J. (2001). Leaf age affects the seasonal pattern of photosynthetic capacity and net ecosystem exchange of carbon in a deciduous forest. *Plant, Cell Environ.*, 24, 571–583.
- Wright, I.J. & Westoby, M. (2003). Nutrient concentration, resorption and lifespan: leaf traits of Australian sclerophyll species. *Funct. Ecol.*, 17, 10–19.
- Wright, I.J., Reich, P.B., Westoby, M., Ackerly, D.D., Baruch, Z., Bongers, F. *et al.* (2004). The worldwide leaf economics spectrum. *Nature*, 428, 821–827.
- Wright, I.J., Reich, P.B., Cornelissen, J.H.C., Falster, D.S., Groom, P.K., Hikosaka, K. *et al.* (2005). Modulation of leaf economic traits and trait relationships by climate. *Glob. Ecol. Biogeogr.*, 14, 411–421.
- Wu, J., Albert, L.P., Lopes, A.P., Restrepo-Coupe, N., Hayek, M., Wiedemann, K.T. *et al.* (2016). Leaf development and demography explain photosynthetic seasonality in Amazon evergreen forests. *Science*, 351, 972–976.
- Wu, J., Chavana-Bryant, C., Prohaska, N., Serbin, S.P., Guan, K., Albert, L.P. *et al.* (2017a). Convergence in relationships between leaf traits, spectra and age across diverse canopy environments and two contrasting tropical forests. *New Phytol.*, 214, 1033–1048.
- Wu, J., Serbin, S., Xu, X. *et al.* (2017b). The phenology of leaf quality and its within-canopy variation is essential for accurate modeling of photosynthesis in tropical evergreen forests. *Glob Change Biol.*, 00, 1–14. <https://doi.org/10.1111/gcb.13725>
- Xu, L. & Baldocchi, D.D. (2003). Seasonal trends in photosynthetic parameters and stomatal conductance of blue oak (*Quercus douglasii*) under prolonged summer drought and high temperature. *Tree Physiol.*, 23, 865–877.
- Xu, X., Medvigy, D., Powers, J.S., Becknell, J.M. & Guan, K. (2016). Diversity in plant hydraulic traits explains seasonal and inter-annual variations of vegetation dynamics in seasonally dry tropical forests. *New Phytol.*, 212, 80–95.

SUPPORTING INFORMATION

Additional Supporting Information may be found online in the supporting information tab for this article.

Editor, Josep Penuelas

Manuscript received 13 February 2017

First decision made 20 March 2017

Second decision made 23 May 2017

Manuscript accepted 31 May 2017